



## Diagnostic Value Of Dynamic Magnetic Resonance Urography In Childhood Obstructive Kidney Diseases

### Çocukluk Dönemi Obstrüktif Böbrek Hastalıklarında Dinamik Manyetik Rezonans Ürografinin Tanı Değeri

Zafer Özmen<sup>1</sup>, Fatma Aktaş<sup>1</sup>, İlkyay Koray Bayrak<sup>2</sup>, Serdar Savaş Gül<sup>3</sup>, Türkay Yalın<sup>2</sup>

<sup>1</sup> Gaziosmanpaşa Üniversitesi Tıp Fakültesi Radyoloji Anabilim Dalı Tokat/Türkiye.

<sup>2</sup> Ondokuz Mayıs Üniversitesi Tıp Fakültesi Radyoloji Anabilim Dalı Samsun/Türkiye.

<sup>3</sup> Gaziosmanpaşa Üniversitesi Tıp Fakültesi Nükleer Tıp Anabilim Dalı Tokat/Türkiye.

#### ÖZ

**Amaç:** Bu çalışmanın amacı, pediatrik üriner sistem hastalıklarının tanısında dinamik manyetik rezonans ürografi (MRÜ)'nin fonksiyonel olarak tanı değerini araştırmak ve obstrüktif patolojilerde obstrüksiyonun derecesinin belirlenmesinde dinamik MRÜ'nin doğruluğunu ortaya koymaktır.

**Materyal ve Metod:** Çalışmaya diüretik renal sintigrafi (DRS)'den önce veya sonra dinamik MRÜ ile değerlendirilen toplam 33 hasta dahil edildi. Hastaların yaşları 1 ay ile 18 yıl (ortalama yaş=7.03 yıl) arasında değişmekteydi. Obstrüksiyonun tanısında standart test olarak DRS kabul edilerek, dinamik MRÜ'nin sensitivite, spesifite, pozitif prediktif değeri ve negatif prediktif değeri hesaplandı.

**Bulgular:** Dinamik MRÜ ve DRS sonuçları arasında fonksiyonel olarak farklılık bulunup bulunmadığını araştırmak için bağımlı gruplarda t testi yapıldı. Split renal fonksiyon açısından dinamik MRÜ ve DRS sonuçları arasında istatistiksel olarak anlamlı farklılık saptanmadı (p=0.978).

**Sonuç:** Çalışmamızda dinamik MRÜ ve DRS sonuçları arasında renal fonksiyonların değerlendirilmesi bakımından çok güçlü ve yüksek bir tutarlılık ve uyum saptadık. Dinamik MRÜ'nin eksresyon açısından normal ve anormal böbrekleri ayırtetmedeki etkinliğini %100 olarak saptadık.

**Anahtar Kelimeler:** Dinamik manyetik rezonans ürografi, diüretik renal sintigrafi, böbrek, obstrüksiyon

#### ABSTRACT

**Objective:** The aim of this study was to investigate the functional value of dynamic magnetic resonance urography (MRU) for the diagnosis of pediatric urinary system diseases, to establish the accuracy of dynamic MRU in determination of obstructive pathologies.

**Materials and methods:** A Total of 33 patients that were evaluated with diuretic renal scintigraphy (DRS) either before or after dynamic MRU examination were included in the study. Their age varied from 1 month to 18 years (mean age was 7.03 years). Accepting DRS as the standard test for diagnosis of obstruction, sensitivity, specificity, and positive predictive and negative predictive values of dynamic MRU were calculated.

**Results:** In order to find whether there was a functional difference between dynamic MRU and DRS measurement results, dependent t-test for paired samples was used. There was no statistically significant difference between (p = 0.978) in split renal function(SRF) results which calculated from dynamic MRU and DRS examinations.

**Conclusions:** We found a very strong and highly significant correlation and consistency between dynamic MRU and DRS methods in terms of evaluation of renal functions. Dynamic MRU is 100% effective for discrimination of normal and abnormal kidneys in terms of excretion.

**Keywords:** Dynamic magnetic resonance urography, diuretic renal scintigraphy, kidney, obstruction



## INTRODUCTION

Diagnostic methods used in the evaluation of childhood urinary system diseases include excretory urography (EU), voiding cystourethrography (VCUG), ultrasonography (USG), contrast/non-contrast computed tomography (CT) and diuretic renal scintigraphy (DRS). However, the diagnosis of urinary system diseases is generally not made based on a single method, and additional examinations lead to increased cost and time loss. Magnetic resonance urography (MRU) has become one of the most frequently used imaging methods, due to its problem solving and non-invasive evaluation of kidney structure, lack of ionized radiation or iodinated contrast material usage, ability to detect urinary system obstructions and diagnose congenital anomalies of the urinary system and other renal diseases (1,2,3,4,5,6,7). Currently, two different techniques are being used in MRU. The first technique, T2 weighted (W) MRU (also known as static-fluid MRU) is generally used for anatomical evaluation of the urinary system. The second technique, T1W MRU (known as contrast excretory MRU or dynamic MRU) provides both anatomical and functional evaluation of the kidneys (2,3,4).

The aim of this study was to investigate the functional value of dynamic MRU for: 1) the diagnosis of pediatric urinary system diseases, 2) the detection of obstructive pathologies of the urinary system, and 3) to establish the accuracy of dynamic MRU in determination of the degree of obstruction in obstructive pathologies.

## MATERIALS AND METHODS

### Patients

Dynamic MRU examination was performed in a total of 96 patients who were referred to Radiodiagnostic Department. These patients had a preliminary diagnosis of urinary system diseases such as ureteropelvic junction obstruction, hypoplastic kidney, and

vesicoureteral reflux (VUR). Sixty-three patients that were not evaluated by DRS, either before or after dynamic MRU examination, were not included the study. A Total of 33 patients that were evaluated with DRS by the Nuclear Medicine Department either before or after dynamic MRU examination (interval between the two examinations varying from 1 day to 1 week) were included in the study.

Age, sex, complaints, and the age at disease onset were recorded in all patients. Seventeen (51%) patients were female and 16 (49%) were male. Their age varied from 1 month to 18 years (mean age was 7.03 years). The distribution of sex and mean age among patients are given in **Table 1**. Patient consent forms were obtained from relatives of patients. However, no ethics committee approval was required because no additional treatment was performed and / or no contrast agent was used except for the contrast agent used routinely.

**Table 1.** Distribution of sex and mean age among patients

	Number of Patients (n)	Age Range	Mean Age
Female	16 (%49)	1 month - 16 years	8,6 years
Male	17 (%51)	3 month -18 years	5,46 years
Total	33 (%100)	1 month -18 years	7,03 years

### Patient preparation

In order to hydrate the patients, intravenous normal saline infusion (0.5-1 mg/kg) was performed at least 30 minutes prior to examination. Because low dose furosemide (0.3 mg/kg) was to be administered, those who could cooperate were asked to urinate before the examination. Laxatives and anti-peristaltic agents were not used.

For optimum patient cooperation during breath-holding protocol, 18 patients at childhood or adolescent periods between the

ages of 7-18 years were informed about the procedure before the examination. However, sedation was required in 15 patients (aged 1 month and 6 years) before initiating dynamic MRU examination since they were not able to comply with breath-holding procedure. Sedation was provided with oral or rectal chloral hydrate (5 mg/kg), which was administered 30 minutes before dynamic MRU. Sedated patients were monitored for tissue oxygenation and cardiac rhythm throughout the examination.

### MRU procedure

Examinations were performed in the supine position using a phase aligned body coil in a device with 1.5 T magnetic field power (Magnetom, Symphony–Quantum, Siemens, Erlangen, GERMANY). The examination was initiated with a 2 dimensional (D) T2W steady state free precession (SSFP) axial and coronal sequence using FOV sufficient to include all abdomen. Subsequently, FOV wide enough to cover the entire urinary system was used and

coronal 3D T1W fast low angle shot (flash) sequence was obtained. The thickness of the examination plan was set to include 1 cm back of the posterior border of the kidney and 1 cm front of the aorta. Then, furosemide (0.3 mg/kg) was administered intravenously with a maximum dose of 20 mg. Three minutes after administration of the diuretic substance, 0.1 mmol/kg Gd–DTPA (Magnevist, Schering, Berlin, Germany) was administered at 0.8 ml/sec from the antecubital vein using a pump injector (Misissippi, Ulrich Medizintechnik, Germany). Then, coronal 3D T1W flash sequence was repeated 4 times, consecutively. Scan time for each sequence was approximately 18 seconds. These sequences were repeated at 120<sup>th</sup>, 300<sup>th</sup>, 420<sup>th</sup>, and 540<sup>th</sup> seconds. If the excretion of contrast material through kidneys was delayed, the procedure was extended and the sequences were repeated with 2 minutes intervals. Maximum duration of the procedure was 25 minutes. Parameters of the sequences used during the examination are given in **Table 2**.

**Table 2.** Sequence parameters used in dynamic MRU

	TR/TE	Flip Angle	FOV (cm)	Avarage	Slice number	Slice thickness (mm)	Matrix	Examination time (sec)
Coronal /Axial 2D T2W SSFP	4,3/2,1	78	30-35	1	14	3	256x256	22
Coronal 3D T1W flash	3.0/1.2	40	28-30	1	60	0,75	256x256	18

### Determination of renal functions and excretion degree

All flash 3D sequences transferred to Siemens Leonardo (Siemens Medical Solutions, Forchheim, Germany) workstation. Mean Curve program, one of the special computer software, was used for the image analysis. In all coronal 3D T1W flash series,

ROIs were drawn to cover both kidney parenchyma and whole kidney (Fig 1).

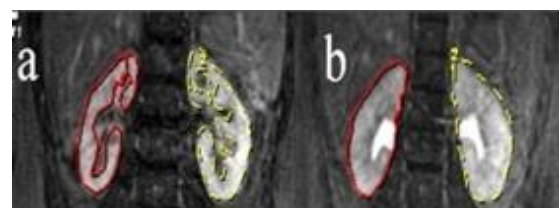


**Fig 1.** a) Renal parenchyma, and b) ROI areas covering whole kidney volume in normal kidneys.



Average ROI area and pixel count calculated from parenchyma and the whole kidney were recorded separately at both kidneys. For each kidney, signal intensities at the ROI area from the sequences obtained at 18<sup>th</sup>, 36<sup>th</sup>, 54<sup>th</sup>, 72<sup>nd</sup>, 120<sup>th</sup>, 300<sup>th</sup>, 420<sup>th</sup>, and 540<sup>th</sup> seconds were recorded.

By plotting the signal intensities at the ROI areas against time, the average intensity-time curves were created for both.

ROI areas calculated at both kidneys, and the average signal intensities at each sequence were entered in Microsoft Office Excel program and a standardized relative intensity-time curve was created similar to average intensity-time curve in order to eliminate possible confounders originating from coil position and parenchymal intensity differences between both kidneys. A standardized relative intensity-time curve was obtained for each sequence by calculating the proportion of renal parenchyma intensity after contrast injection (Si) to parenchyma intensity before contrast injection (So) (Si-So/So).

In our study, we only used standardized relative intensity-time curves created from ROI's drawn to parenchyma in order to calculate split renal function (SRF) as mentioned in previous reports (8,9,10).

In dynamic MRU intensity-time curves, a normal kidney has three phases similar to the activity-time curves in DRS. These phases correspond to the first (vascular), second (parankimal) and third (excretory) segments in dynamic MRU curves (**Fig 2**).

The vasculature phase begins 20-25 seconds after the contrast agent injection and reaches a maximum peak with a very steep incline. The parenchymal phase begins at 40-60th seconds after the vasculature phase and reaches a maximum peak at 130-150th seconds with a slower curve (11). The parenchymal phase forms the second segment of the intensity-time curve. This segment is used to

calculate the renal function in dynamic MRU and DRS (12,13,14). With the end of the parenchymal phase, excretion phase forming the third segment starts. In intensity-time curves, the maximum peak point of the second segment is considered to be the beginning of the third segment. The third segment falls suddenly and concavely below the starting point of the second segment. This segment is used to calculate the excretion of the kidneys in the dynamic MRU (12) and DRS (11).

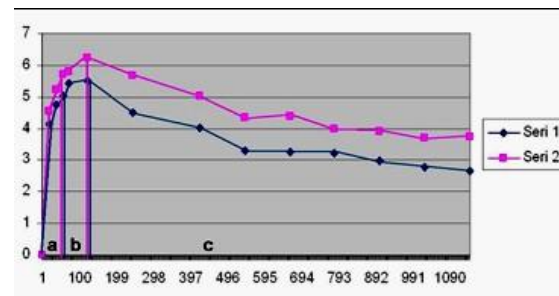


**Fig 2.** a) First (vascular), b) Second (parenchymal) and c) Third (excretory) segments in standardized relative intensity-time curves in normal kidneys.

SRF was calculated by determining the ratio of two parameters between the right and left kidneys. These parameters were the 'area under the second segment of the standardized intensity over the time curve' and the 'volume of functional tissue' (15). Functional tissue volume corresponds to the volume of tissue remaining in the ROIs we have drawn on both kidney parenchyma. Then, the 'functional tissue volume' and the 'area under the second segment of standardized intensity over time curve' were proportioned to the contralateral kidney to calculate SRF for each kidney. Thus, the percentage of each kidney's contribution in total renal function was determined. In order to create standardized relative intensity-time curve that is required to evaluate urinary excretion with dynamic MRU, ROI area covering whole kidney (renal parenchyma + renal pelvis) was used as described in previous reports (8,9,10). Presence of obstruction to urinary excretion was determined via demonstration of presence or absence of the decline that is expected to occur at the third

segment of standardized relative intensity-time curve after furosemide administration. The excretion level of the kidneys by the shape of the third segment curve is shown in **Table 3** (15).

**Table 3.** Classification of kidneys according to excretion grades

<b>Grade I</b>	Sudden and concave fall of the third segment (normal)
<b>Grade II</b>	Progressive increasing occurs in the third segment curve and there is no diuretic response (obstructive pattern)
<b>Grade IIIa</b>	The third segment curve initially rises, then provides adequate diuretic response and falls to its normal level. Completely emptied dilate, non-obstructive pattern (functional agent stasis)
<b>Grade IIIb</b>	The third segment curve initially rises, then provides adequate diuretic response and falls to its normal level. Completely emptied dilate, non-obstructive pattern (functional agent stasis)
<b>Grade IV</b>	Very little or no contrast agent in the collecting system due to significant decrease in the concentration ability of the kidneys (Kidneys are weak or nonfunctional)

Patients' DRS examinations were evaluated by Nuclear Medicine Department in independent and blind fashion. Dynamic renography was obtained after an intravenous injection of 7.4 MBq/kg Technesium-99m mercapto-acetyltriglycine (Tc-99m MAG-3) with a minimum dose of 15 MBq and a maximum dose of 100 MBq. Images were acquired at 2 s/frame for 24 frames, 15 s/frame for 16 frames and 30 s/frame for 40 frames (64×64 matrix) with a large field of gamma camera equipped with a low-energy all-purpose parallel-hole collimator. Energy setting was done according to a photopeak of 140 keV with a 20% symmetric window. MAG-3 SRF was calculated using 2 different time intervals (1–2 and 2–3 min). SRF values were obtained on a manually drawn kidney ROI over the kidney. A bean-shaped renal ROI was used to exclude the collecting system. A

perirenal C-type region of background activity was used for background subtraction. SRF values were obtained using an area under the curve method. Present dynamic MRU results were compared with DRS, which is referred as the standard method.

### Statistical evaluation

Accepting DRS as the standard test for diagnosis of obstruction, sensitivity, specificity, and positive predictive and negative predictive values of dynamic MRI were calculated.

In order to find whether there was a functional difference between dynamic MRU and DRS measurement results, dependent t-test for paired samples was used. To evaluate the correlation between two applications, Pearson correlation analysis was performed. Statistical analyses were carried out on Statistical Package for Social Science for Windows 11.5 (SPSS - 11.5) software program.

### RESULTS

Dynamic MRU was evaluated in a total of 33 patients and 64 kidneys. Two patients had a single kidney. 12 of the renal pathologies were bilateral while 21 were unilateral. 27 of the kidneys had pelvicalyceal ectasia and in 14 of them, pelvicalyceal ectasia was accompanied by ureter dilatation. The duplex collecting system was present in five kidneys, and in 1 of these, the duplex collecting system ended in the ureteropelvic junction. Renal pelvis duplication was also accompanied by ureter duplication in the other 4 kidneys. Atrophy-hypoplasia was detected in five kidneys. 3 kidneys had multiple cysts. One of the kidneys with cysts was also atrophic. In one kidney, malrotation was detected along with ectasia.

### Evaluation of SRF results

Dependent t-test for paired samples was performed in order to determine the difference in SRF results calculated from dynamic MRU and DRS examinations. There was no

statistically significant difference between measurements ( $p = 0.978$ ). It was found that dynamic MRU was safe for determination of SRF.

Pearson correlation analysis was performed to determine the association between dynamic MRU and DRS measurements. There was a very strong and highly significant correlation between measurement results ( $r=0.99$ ,  $p=0.000$ ). SRF from dynamic MRU showed highly significant correlation with SRF from DRS ( $r=0.99$ ,  $p=0.000$ ). Despite this high correlation, the variation between the results of dynamic MRU and DRS in 4 patients was more evident than in the other patients. There was a 6-11% variation in the SRF values calculated in dynamic MRU and DRS in these patients. Distribution of age, sex, and SRF based on dynamic MRU and DRS among these four patients are given in **Table 4**.

**Table 4.** Distribution of age and sex, and split renal functions based on dynamic MRU and DRS among four patients.

Patient no	Age (Years)	Sex	SRF (%)		SRF (%)	
			Dynamic MRU (%)		DRS (%)	
			Right	Left	Right	Left
2	6	F	88,5	11,5	97	3
10	5	M	43	57	36	64
18	5	F	71,4	28,6	77	23
24	14	M	72	28	78	22

The results were pretty similar in the remaining 56 kidneys of 29 patients (**Fig 3**).

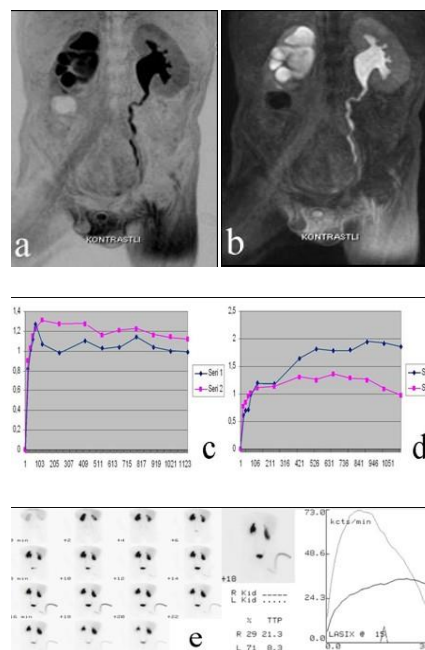


**Fig 3.** In normal flash 3D MIP coronal images of a 7 years old male patient (**a,b**). Right kidney parenchyma is observed thinner, and pelvicalyceal structures have grade IV ectasia. Right ureter is not observed as there is no sufficient contrast material passage. Left pelvicalyceal structures have grade III ectasia, and left ureter is observed to have normal width. Contrast material passage in to the ureter is seen. In functional evaluation, SRF calculated with dynamic MRU are (**c**) 24% for right kidney and 76% for left kidney; and SRF calculated with DRS are (**e**) 29% for right kidney and 71% for left kidney. In evaluation of excretion, right kidney is determined to have obstruction (grade II) in dynamic MRU (**d**) and DRS (**e**). Excretion at left kidney is evaluated as functional stasis (grade IIIa) in dynamic MRU (**d**) and DRS (**e**).

### Evaluation of renal excretion

Kidneys were classified in terms of degree of excretion from grade I to grade IV. According to this classification, 33 kidneys (52%) were grade I, 16 kidneys (25%) were grade II, 6 kidneys (9.4%) were grade IIIa, 3 kidneys (4.6%) were grade IIIb, and 6 kidneys (9.4%) were Grade IV. These results obtained from dynamic MRU were compared to DRS, which is regarded as the standard method. **Table 5** shows percentage distribution of excretion grades based on dynamic MRU and DRS methods.

When DRS was accepted as the standard method, dynamic MRU could discriminate normal and pathological kidneys by 100%. Therefore, sensitivity, specificity, and positive and negative predictive values of dynamic MRU for discrimination of normal and pathological kidneys were all 100%.

**Table 5.** Percentage distribution of excretion types based on dynamic MRU and DRS

	Dynamic MRU		DRS	
	Number of kidney	%	Number of kidney	%
<b>Grade I</b> (Normal)	33	51,6	33	51,6
<b>Grade II</b> (Obstruction)	16	25	13	20,3
<b>Grade IIIa</b> (Functional stasis)	6	9,4	9	14,1
<b>Grade IIIb</b> (Borderline obstruction)	3	4,6	3	4,6
<b>Grade IV</b> (Atrophy)	6	9,4	6	9,4
<b>Total</b>	64	100,0	64	100,0

DRS method could correctly identify 13 of the 16 kidneys that were shown to have obstruction with dynamic MRU method. For the remaining 3 kidneys, DRS showed functional stasis in 2 kidneys and borderline obstruction in 1 kidney. Regarding obstruction, sensitivity of dynamic MRU was 100%, specificity was 94%, positive predictive value was 81%, and negative predictive value was 100%. Since the number of cases was not sufficient regarding borderline obstruction, statistical analysis was not performed. **Table 6** shows sensitivity, specificity, positive and negative predictive value of dynamic MRU for detection of obstruction.

Based on dynamic MRU, functional stasis was detected in 6 kidneys. All of them were confirmed with DRS. However, 9 kidneys were reported to have functional stasis based on DRS. Based on the dynamic MRU, two of them were defined as obstruction and one of them was defined as borderline obstruction.

**Table 6.** Sensitivity, specificity, positive and negative predictive value of dynamic MRU

	Sensitivity (%)	Specificity (%)	Positive predictive value (%)	Negative predictive value (%)
<b>Grade I</b> (Normal)	100	100	100	100
<b>Grade II</b> (Obstruction)	100	94	81	100
<b>Grade IIIa</b> (Functional stasis)	67	100	100	95
<b>Grade IIIb</b> (Borderline obstruction)	--	--	--	--
<b>Grade IV</b> (Atrophy)	100	100	100	100

Sensitivity of MRU regarding detection of functional stasis was 67%, specificity was 100%, positive predictive value was 100%, and negative predictive was 95%. Six kidneys were determined to be atrophic based on dynamic MRU, and they were confirmed with DRS. Sensitivity, specificity, and positive and negative predictive values of dynamic MRU for detection of atrophy was all found as 100%.

## DISCUSSION

Dynamic MRU is one the best known methods for morphological and functional evaluation of urinary system (8,16). It is especially very helpful in the follow-up of patients with ureteropelvic junction obstruction (17). Correct calculation of renal functions in dynamic MRU depends on several factors. The most important of these factors are renal parenchymal volume and voxel function (11). Inaccurate measurement of any of these components might lead to inaccurately calculated SRF. In our study, we used ROI's that covered all parenchyma in coronal plane, as mentioned in previous reports. By adjusting these ROI to match localization of kidney at the same section in all sequences, we calculated renal functional tissue area. Utilization of this method is significant, since



the kidney has an irregular surface. A shortcoming of this method is its dependence on the operator, as it is performed manually and is time consuming. Furthermore, accurate calculation of the volume might be difficult in case of large space-occupying lesions within the parenchyma (e.g. polycystic kidney disease). In our study, we did not find significant difference between SRF results calculated from dynamic MRU and DRS in one having multiple cysts in both kidneys and one having multiple cysts at left kidney. Studies that are related to evaluation of renal functions and excretion with dynamic MRU have found very similar results to evaluation with DRS (18). Rohrschneider et al. (19) had similar results with both dynamic MRU and DRS for determination of SRF and excretion of kidneys in their study with 62 pediatric patients using 0.5T MR and 0.1 mmol/kg Gd administration.

Our study showed a very strong and highly significant correlation between dynamic MRU and DRS for measurement of SRF ( $r=0.99$ ,  $p=0.00$ ). Nonetheless, the difference in SRF measurement was more prominent in 4 patients. In one of these patients, dynamic MRU showed normal right kidney and right ureter but grade III ectasia at left kidney. Left ureter was normal. There were unilateral atrophy in the remaining three patients, and both ureters were normal. In the case with ectasia, the reason why SRF was calculated different based on dynamic MRU compared to DRS was thought to be inaccurate positioning of ROI area due to large hydronephrotic areas. For atrophic kidneys, the deviation in SRF was thought to originate from the difficulty in measurement of ROI area in atrophic kidneys and also due to the fact that small changes in measurement of ROI area lead to great changes in SRF.

When evaluated in terms of renal excretion, dynamic MRU and DRS results were inconsistent in 4 cases in our study. Dynamic MRU showed greater obstruction

than the actual in these cases. In three individual cases, dynamic MRU showed obstruction, whereas DRS showed functional stasis in two of them and borderline obstruction in one of them. The other case was determined to have borderline obstruction with dynamic MRU, but reported as functional stasis with DRS. In our study, we think higher grades detected in 4 patients, which were observed greater than the actual with dynamic MRU, are due to elevated baseline in dynamic MRU because of differences in contrast materials used in both examinations and limitation in examination time in dynamic MRU.

Recommended approach for comparison of renal functions and urinary system obstruction with DRS is to calculate renal function quantitatively and to determine the difference between obstruction grades. We calculated renal functions quantitatively in our study, and obstruction was graded using both methods. SRF can be evaluated precisely and accurately with dynamic MRU (12). Grattan-Smith et al.(20) and Perez-Brayfield et al.(21) showed correlation between DRS and dynamic MRU methods in terms of evaluation of SRF.

Dynamic MRU gives the ability to evaluate the urinary system in anatomical, functional and excretional terms in a single examination (22,23). One of its most important features is that it does not make use of ionized radiation. As it enables vascular, anatomical and functional evaluation without using ionized radiation, dynamic MRU examination is necessary especially in infants and children (19). When patients with definite urinary system stenosis are treated conservatively, they are followed up with consecutive examinations to evaluate renal function and structure until the end of the treatment or until operation time. Follow-up of these patients is generally performed at least once in a year using USG and DRS. Therefore, it is thought that dynamic MRU can take the place of DRS for complete imaging of the urinary system in young



patients when consecutive examinations are necessary, as it does not make use of ionized radiation.

However, despite all its advantages, there are some limitations of dynamic MRU. The major one is determination of ROI area. Proper determination of ROI area can be difficult due to presence of motion artifacts. Determination of ROI area is important regarding evaluation of excretion and function, and it requires experience. Furosemide administration together with sedation creates a high risk for bladder distention. An extremely full bladder can inhibit urinary drainage. This inhibition can lead to obstruction being observed inaccurately greater than the actual. This inhibition is also well known for DRS (24). Another potential handicap in the evaluation of SRF arises from the time intervals in MR images of the patient. MR images with short time intervals are preferred for SRF measurement, because critical information can be overlooked with long time intervals. Real intensity peaks may be overlooked, leading to falsely low SRF calculations. In our study, the sequences were obtained at 18<sup>th</sup>, 36<sup>th</sup>, 54<sup>th</sup>, 72<sup>nd</sup>, 120<sup>th</sup>, 300<sup>th</sup>, 420<sup>th</sup>, and 540<sup>th</sup> seconds. In case there was a suspicion of obstruction, the procedure time was extended. For patients who were suspected to have obstruction, the scanning procedure was extended until 24<sup>th</sup> minute maximum, with 120 seconds intervals. The time interval between the initial four sequences was 18 seconds, and the interval between the sequences were adequate and consistent with the literature (25). Another limitation of dynamic MRU depends on the contrast agent used. The gadolinium-based contrast agent is preferred to evaluate renal function. The reason for this is that these substances are filtered through the glomerulus. They are not exposed to significant tubular secretion or reabsorption and are minimally bound to plasma proteins. Two particular contrast agents that meet these criteria are Gadopentetate dimeglumine (Magnevist; Bayer HealthCare, Whippany, NJ) and

gadoteridol (Prohance; Bracco Diagnostics, Monroe Township, NJ). That's why we used Gadopentetate dimeglumine as a contrast agent in our study. However, children with acute kidney injury or chronic kidney disease and patients with an estimated glomerular filtration rate less than 30 mL/min/1.73 m<sup>2</sup> have a potential risk for nephrogenic systemic fibrosis (NSF), a disease associated with gadolinium-based contrast agents (26,27,28,29). NSF is defined as a systemic, sclerosing skin disease that resembles sclerodema in patients with renal insufficiency. For this reason, it is advisable to evaluate the rate of serum creatinine concentration and glomerular filtration before application of contrast agent (30). Fortunately, pediatric nephrogenic systemic fibrosis is very rare, with only 23 documented cases of September 2012 (19,21b). Some institutions recommend the use of macrocyclic contrasting agents to minimize NSF risk (29,30).

In conclusion, we found a very strong and highly significant correlation and consistency between dynamic MRU and DRS methods in terms of evaluation of renal functions. Dynamic MRU is 100% effective for discrimination of normal and abnormal kidneys in terms of excretion. However, with regard to classification of abnormal kidneys within themselves, dynamic MRU might cause the degree of obstruction to be evaluated greater than actual in some patients, when compared DRS. Dynamic MRU has revolutionized imaging of urinary system in children by providing good quality anatomical information, quantitative functional evaluation and determination of degree of excretion without making use of ionized radiation. It has a great potential owing to these properties.

**REFERENCES**

1. Dickerson EC, Dillman JR, Smith EA, Di Pietro MA, Lebowitz RL, Darge K. Pediatric MR Urography: Indications, Techniques and Approach to Review. *Radiographics* 2015;35(4):1208-30.
2. Levendecker JR, Barnes CE, Zagoria RJ. MR urography: techniques and clinical applications. *Radiographics* 2008;28:23–46.
3. Battal B, Kocaoglu M, Akgun V, Aydur E, Dayanc M, Ilica T. Feasibility of MR urography in patients with urinary diversion. *J Med Imaging Radiat Oncol* 2011;55:542–50.
4. Kocyiğit A, Yuksel S, Bayram R, Yılmaz İ, Karabulut N. Efficacy of magnetic resonance urography in detecting renal scars in children with vesicoureteral reflux. *Pediatr Nephrol* 2014;29:1215–20.
5. Grattan-Smith JD, Little SB, Jones RA. MR urography evaluation of obstructive uropathy. *Pediatr Radiol* 2008;38:49–69.
6. Grattan-Smith JD, Jones RA. MR urography: technique and results for the evaluation of urinary obstruction in pediatric population. *Magn Reson Imaging Clin N Am* 2008;16:643–60.
7. Darge K, Anupindi SA, Jaramillo D. MR imaging of the abdomen and pelvis in infants, children, and adolescents. *Radiology* 2011;261:12–29.
8. Bayrak IK, Ozmen Z, Nural MS, Danaci M. *Korean J Radiol* 2008 Jun;9(3):250-7.
9. Avni F, Bali MA, Regnault M, et al. MR urography in children. *Eur J Radiol* 2002;43:154-66.
10. Kocaoglu M, Bulakbasi N, Ilica AT, Gok F, Tayfun C, Somuncu I. Intravenous contrast-enhanced dynamic MR urography: diagnosis of vesicoureteral reflux during bladder filling with time-signal intensity curves. *J Magn Reson Imaging* 2006;24:349-55.
11. Brown SCW. Nuclear medicine in the clinical diagnosis and treatment of obstructive uropathy. In: Murray ICP, Ellis PJ, eds. *Edinburgh, Scotland: Churchill Livingstone*, 1998; 291-313.
12. Rohrschneider WK, Becker K, Hoffend J, et al. Combined static-dynamic MR urography for the simultaneous evaluation of morphology and function in urinary tract obstruction. II. Findings in experimentally induced ureteric stenosis. *Pediatr Radiol* 2000;30:523-32.
13. Khrichenko D, Darge K. Functional analysis in MR urography—made simple. *Pediatr Radiol* 2010;40(2):182–199.
14. Little SB, Jones RA, Grattan-Smith JD. Evaluation of UPJ obstruction before and after pyeloplasty using MR urography. *Pediatr Radiol* 2008;38:106–124.
15. Teh HS, Ang ES, Weng WC, et al. MR renography using a dynamic gradient-echo sequence and low-dose gadopentetate dimeglumine as alternative to radionuclide renography. *AJR* 2003;181:441-450.
16. Vivier PH, Blondiaux E, Dolores M, Marouveau-Pasquier N, Brasseur M, Petitjean C, Dacher J. *J Radiol* 2009 Jan;90:11-9.
17. Khrichenko D, Darge K. Functional analysis in MR urography—made simple. *Pediatr Radiol* 2010;40(2):182–99.
18. Mazdak H, Karam M, Ghassami F, Malekpour A. Agreement between static magnetic resonance urography and diuretic renal scintigraphy in patients with ureteropelvic junction obstruction after pyeloplasty. *Adv Biomed Res* 2015;4:186.
19. Rohrschneider WK, Haufe S, Wiesel M, et al. Functional and morphologic evaluation of congenital urinary tract dilatation by using combined static-dynamic MR urography: findings in kidneys with a single collecting system. *Radiology* 2002;224:683–94.
20. Grattan-Smith JD, Perez-Bayfield MR, Jones RA, et al. MR imaging of kidneys: functional evaluation using F-15 perfusion imaging. *Pediatr Radiol* 2003;33:293-304.
21. Perez-Brayfield MR, Kirsch AJ, Jones RA, Grattan-Smith JD. A prospective study comparing ultrasound, nuclear scintigraphy and dynamic contrast enhanced magnetic resonance imaging in the evaluation of hydronephrosis. *J Urol* 2003;170:1330-4.
22. Jones RA, Perez-Brayfield M, Kirsch AJ, Grattan-Smith JD. Renal transit time using MR urography: a new classification of obstructive uropathy in children. *Radiology* 2004;233:41-50.
23. Battal B, Kocaoglu M, Akgun V, Ince S, Gök F, Taşar M. Split-bolus MR urography: synchronous visualization of obstructing bolus MR urography: synchronous vessels and collecting system in children. *Diagn Interv Radiol*. 2015 Nov-Dec;21(6):498-502.
24. Rohrschneider WK, Hoffend J, Becker K, et al. Combined static-dynamic MR urography for the simultaneous evaluation of morphology and function in urinary tract obstruction. I. Evaluation of the normal status in an animal model. *Pediatr Radiol* 2000;30:511-22.
25. Jones RA, Easley K, Little SB, et al. Dynamic contrast-enhanced MR urography in the evaluation of pediatric hydronephrosis: Part 1, functional assessment. *Am J Roentgenol* 2005; 185:1598-607.
26. Nardone B, Saddleton E, Laumann AE, et al. Pediatric nephrogenic systemic fibrosis is rarely reported: a RADAR report. *Pediatr Radiol* 2014;44(2):173–180.
27. Weinreb JC. Impact on hospital policy: Yale experience. *J Am Coll Radiol* 2008;5(1):53–6.
28. Altun E, Martin DR, Wertman R, Lugo-Somolinos A, Fuller ER, Semelka RC. Nephrogenic systemic fibrosis: change in incidence following a switch in gadolinium agents and adoption of a gadolinium policy-report from two U.S. universities. *Radiology* 2009;253(3):689–96.
29. Martin DR. Nephrogenic systemic fibrosis. *Pediatr Radiol* 2008;38:125–9.
30. Schwartz GJ, Muñoz A, Schneider MF, et al. New equations to estimate GFR in children with CKD. *J Am Soc Nephrol* 2009;20(3):629–37.